Water Research 123 (2017) 113–123

Contents lists available at ScienceDirect

Water Research

journal homepage: www.elsevier.com/locate/watres

Inactivation of pathogenic microorganisms in freshwater using HSO_5^-/UV-A LED and HSO_5^-/M^{n+}/UV-A LED oxidation processes

Jorge Rodríguez-Chueca [a, b], Tatiana Silva [c], José R. Fernandes [d, e], Marco S. Lucas [a, f, *], Gianluca Li Puma [f], José A. Peres [a], Ana Sampaio [c]

[a] Centro de Química de Vila Real, Departamento de Química, UTAD - Universidade de Trás-os-Montes e Alto Douro, Quinta de Prados, 5000-801, Vila Real, Portugal
[b] Department of Chemical and Environmental Technology, ESCET, Universidad Rey Juan Carlos, C/ Tulipán s/n, 28933, Móstoles, Madrid, Spain
[c] Centro de Investigação e de Tecnologias Agroambientais e Biológicas (CITAB), Departamento de Biologia e Ambiente, UTAD, Quinta de Prados, 5000-801, Vila Real, Portugal
[d] Departamento de Física, UTAD - Universidade de Trás-os-Montes e Alto Douro, Quinta de Prados, 5000-801, Vila Real, Portugal
[e] INESC-TEC, Rua do Campo Alegre, 687, 4169-007, Porto, Portugal
[f] Environmental Nanocatalysis & Photoreaction Engineering, Department of Chemical Engineering, Loughborough University, Loughborough, LE11 3TU, United Kingdom

ARTICLE INFO

Article history:
Received 20 March 2017
Received in revised form
6 June 2017
Accepted 7 June 2017
Available online 10 June 2017

Keywords:
Peroxymonosulphate
Microorganism inactivation
UV-A LED
Kinetic modelling
PMS/M^{n+}/UV-A LED bacterial inactivation mechanism

ABSTRACT

Freshwater disinfection using photolytic and catalytic activation of peroxymonosulphate (PMS) through PMS/UV-A LED and PMS/M^{n+}/UV-A LED [M^{n+} = Fe^{2+} or Co^{2+}] processes was evaluated through the inactivation of three different bacteria: *Escherichia coli* (Gram-negative), *Bacillus mycoides* (sporulated Gram-positive), *Staphylococcus aureus* (non-sporulated Gram-positive), and the fungus *Candida albicans*. Photolytic and catalytic activation of PMS were effective in the total inactivation of the bacteria using 0.1 mM of PMS and M^{n+} at neutral pH (6.5), with *E. coli* reaching the highest and the fastest inactivation yield, followed by *S. aureus* and *B. mycoides*. With *B. mycoides*, the oxidative stress generated through the complexity of PMS/M^{n+}/UV-A LED combined treatments triggered the formation of endospores. The treatment processes were also effective in the total inactivation of *C. albicans*, although, due to the ultrastructure, biochemistry and physiology of this yeast, higher dosages of reagents (5 mM of PMS and 2.5 mM of M^{n+}) were required.

The rate of microbial inactivation markedly increased through catalytic activation of PMS particularly during the first 60 s of treatment. Co^{2+} was more effective than Fe^{2+} to catalyse PMS decomposition to sulphate radicals for the inactivation of *S. aureus* and *C. albicans*.

The inactivation of the four microorganisms was well represented by the Hom model. The Biphasic and the Double Weibull models, which are based on the existence of two microbial sub-populations exhibiting different resistance to the treatments, also fitted the experimental results of photolytic activation of PMS.

1. Introduction

Water disinfection is a complex process which is highly dependent on environmental factors and target microorganisms. *Escherichia coli* is a common indicator of fecal contamination in the analyses of water and wastewater (Parés and Juárez, 2002). This facultative anaerobic gram-negative bacteria is catalase positive and inhabits the intestinal tract of humans and other vertebrates and can be responsible for gastrointestinal diseases. In contrast, *Bacillus mycoides* is neither pathogenic nor a toxin producer. *B. mycoides* is a catalase positive, rod-shaped gram-positive bacteria, which has a typical rhizoid growth on solid media is catalase positive and able to ferment sugars such as glucose and maltose. It is a ubiquitous bacterium commonly found on plants, in soil, water, air, and decomposing plant tissue and frequently contaminates food, mainly vegetables. Under stress conditions *B. mycoides* forms

* Corresponding author. Centro de Química de Vila Real, Departamento de Química, UTAD - Universidade de Trás-os-Montes e Alto Douro, Quinta de Prados, 5000-801, Vila Real, Portugal.
E-mail addresses: m.p.lucas@lboro.ac.uk, mlucas@utad.pt (M.S. Lucas).

http://dx.doi.org/10.1016/j.watres.2017.06.021
0043-1354/

endospores, which are resistant to physical and chemical factors such as high temperature, radiation and chemical disinfectants. *Staphylococcus aureus* is a gram-positive bacteria often found on skin, on skin glands, nasal and other mucous membranes, as well as on a wide range of food products such as milk and cheese through contact with workers that carry *S. aureus*. This catalase-positive and toxin producing bacteria is potentially pathogenic and can cause food poisoning when a food handler contaminates food or the food is not properly refrigerated. *Candida albicans* is a commensal fungus with a eukaryotic structure, commonly found in the oral and vaginal mucosa and in the gastrointestinal tract of humans. *C. albicans* lives in 80% of the human population, typically without causing harmful effects. However, excess of this fungus results in candidiasis (Calderone, 2002), causing opportunistic infections in immunocompromised patients, although it is rarely responsible for morbidity or mortality (Douglas, 1988).

Chlorination is the most commonly used disinfection agent worldwide (LeChevallier and Au, 2004) and since its introduction over a century ago, human life expectancy has increased due to the prevention of waterborne diseases previously responsible for high mortality rates. The widespread use of chlorination has occurred as a result of its high rate of disinfection, its residual effect in the water, the low treatment cost, and the ease of handling. However, the generation of disinfection by-products (DBPs) (Rook, 1974) has raised significant concern among water treatment plants and regulators. More than 600 different DBPs have been reported in the literature (Richardson et al., 2007) the majority of which consists of trihalomethanes (THMs), chlorinated acetic acids, chlorinated ketones and halocetonitriles (WHO, 2008). DBPs are associated with public health risks via ingestion, inhalation, and skin absorption (Doederer et al., 2014). The majority of DBPs are a consequence of the chlorination of naturally occurring organic precursors such as humic substances (WHO, 2008; Grellier et al., 2015). Consequently, finding alternative effective mean of water disinfection which simultaneously avoid the generation of disinfection by-products has attracted the attention of many investigators (Venieri et al., 2015; Ferro et al., 2015; Giannakis et al., 2015).

Advanced Oxidation Processes (AOPs) are emerging as effective processes, which combine contaminants oxidation and disinfection. These are based on the generation of highly reactive species with a short lifetime such as hydroxyl radical-based AOPs (HR-AOPs), and sulphate radical-based AOPs (SR-AOPs). SR-AOPs based on sulphate radicals involves the application of chemical oxidants as persulphate salts, for example $Na_2S_2O_8$, $K_2S_2O_8$ and $KHSO_5$ (Wei et al., 2015). Peroxymonosulphate (HSO_5^-; PMS), is the active ingredient of potassium hydrogen monopersulphate ($2KHSO_5 \cdot KHSO_4 \cdot K_2SO_4$). The use of PMS as a disinfectant agent presents some advantages compared to hydrogen peroxide based HR-AOPs. Firstly, the oxidation potential of ($E^{\circ}_{HSO_5^-/HSO_4^-} = 1.82\ V$) is higher than that of hydrogen peroxide ($E^{\circ}_{H_2O_2/H_2O} = 1.78V$), although lower than the potential of the hydroxyl radical ($E^{\circ}_{OH} = 2.80\ V$). Furthermore, in contrast to H_2O_2 which requires special handling, potassium hydrogen monopersulphate is relatively stable at room temperature and easy to handle due to its solid state.

PMS alone is not an efficient disinfectant, but its action is significantly increased when it is catalytically (Eqs. (1)–(3)), thermally or photolytically (Eq. (4)) activated, (Reactions 1–4) (Anipsitakis et al., 2008; Wang et al., 2011; Wang and Chu, 2012).

$$HSO_5^- + M^{n+} \rightarrow SO_4^{\bullet -} + M^{(n+1)+} + OH^- \quad (1)$$
$$\mathrm{M} = Co^{2+},\ Fe^{2+} \text{ and } Ru^{3+}$$

$$HSO_5^- + M^{n+} \rightarrow \left[M^{(n+1)+}(SO_4^{\bullet}) \right]^{n+} + OH^- \quad (2)$$
$$\mathrm{M} = Ce^{3+},\ Mn^{2+},\ Ni^{2+}$$

$$HSO_5^- + M^{(n+1)+} \rightarrow SO_5^{\bullet -} + M^{n+} + H^+ \quad (3)$$
$$\mathrm{M} = Ce^{4+},\ Fe^{3+},\ Mn^{3+}$$

$$HSO_5^- \xrightarrow{h\nu/\Delta} SO_4^{\bullet -} + HO^{\bullet} \quad (4)$$

Different authors have reported the catalytic activation of PMS through different transition metals such as Fe^{2+}, Co^{2+}, and Ni^{2+} (Anipsitakis et al., 2008; Wang and Chu, 2012; Anipsitakis and Dionysiou, 2003), but it is not clear which transition metal best activates PMS. For instance, the coupling of HSO_5^-/Fe^{2+} is one of the most commonly used combination, but presents disadvantages similar to those of the Fenton oxidation process, such as slow regeneration of Fe^{2+} and the production of ferric hydroxide sludge (Wang and Chu, 2012). The alternative coupling HSO_5^-/Co^{2+} presents some advantages in comparison to Fenton treatments, the most relevant of which being that it allows using HSO_5^-/Co^{2+} without pH adjustment (Bandala et al., 2007; Yu et al., 2006), however the toxicity of Co^{2+} is a matter of concern in water treatment.

In this study, the effectiveness of SR-AOPs such as HSO_5^-/UV-A LED and HSO_5^-/M^{n+}/UV-A LED [$M^{n+} = Fe^{2+}$ or Co^{2+}] was assessed as alternative drinking water disinfection processes for the inactivation of a range of target microorganisms including the bacteria *E. coli* (gram-negative), *B. mycoides* (gram-positive endospore producer) and *S. aureus* (a non-endospore forming gram-positive) and the eukaryotic fungus *C. albicans*. The inactivation kinetics of these microorganisms was evaluated by nonlinear regression. This investigation into the disinfection of pathogen germs using PMS/UV-A LED and PMS/M^{n+}/UV-A LED systems contributes to future discussions regarding possible attack mechanisms of sulphate radicals in microbial inactivation.

2. Material and methods

2.1. Microorganisms and chemicals

Wild strains of *E. coli* and *B. mycoides* were isolated from a water well and from soil, respectively, while collection strains of *C. albicans* and *S. aureus* were used (*C. albicans* ATCC 90028; *S. aureus* NCTC 10788/ATCC 6538). *E. coli* quantification was made over the selective culture media Chromocult agar (Merck) and *B. mycoides* and *S. aureus* determinations were carried out over a Luria-Bertani (LB) agar. LB agar was prepared by mixing tryptone (10 g/L; Difco®), NaCl (10 g/L; Merck), yeast extract (5 g/L; Gibco Europe) and agar-agar (1.5%; Merck). *C. albicans* was quantified using the yeast malt extract agar (YMA, Difco®): peptone (5 g/L), yeast extract (3 g/L), malt extract (3 g/L), glucose (10 g/L) and agar-agar (20 g/L).

Fresh liquid cultures were prepared in LB broth (bacteria) or Yeast-Malt broth (yeast) and incubated at 37 °C in a rotary shaker (150 r.p.m.) for 20 h. 1 mL of these microbial suspensions were then added to water samples (500 mL) to obtain microorganisms concentrations ranging from 10^5–10^6 colony-forming units (CFU)/100 mL.

All reagents used were analytical grade. Peroxymonosulphate and the metal catalysts ($CoSO_4 \cdot 7H_2O$ or $FeSO_4 \cdot 7H_2O$) were purchased from Merck® and Panreac, respectively. Sulphuric acid (H_2SO_4 Scharlau) and sodium hydroxide (NaOH Panreac) were used for pH adjustment. UV-A LED radiation was used in combination

with selected reagents to increase the rate of formation of sulphate radicals.

2.2. Disinfection experiments and UV-A LED photo reactor

Freshwater samples (pH = 7.2–7.8; reduction potential (RP) = −0.82 mV; chemical oxygen demand (COD) = 10–15 mg O_2/L; electrical conductivity (EC) = 230–250 μS; and total suspended solids (TSS) = 1–3 mg/L and turbidity = 0.4–1 NTU) were collected from an artificial lake located at the UTAD campus (Vila Real, Portugal). Sampling, handling and storage was carried out following the ISO 5667-3, 2012 protocol.

Photo activation of PMS was carried out in lab-scale batch reactor illuminated with a UV-A LED photo-system consisting of a matrix of 96 Indium Gallium Nitride (InGaN) LEDs lamps (Roithner RLS-UV370E) which illuminated an area of (11 × 7) cm^2. Each LEDs with light peak emission at 370 nm, consumed 80 mW at an applied current of 20 mA. The LED array optical emission was controlled by a pulse width modulation (PWM) circuit, which determined the electric current supplied to each array LED. The square waveform current supplied had two states: 0 mA (LED emission OFF state) and 30 mA (LED emission ON state) and frequency of 350 Hz. The PWM module allows the configuration of the ON state time duration in each cycle between 0 and 100% of the cycle period and, consequently, the emitted average optical power was controlled between 0 and 100 mW. The photon irradiance was measured using a UV enhanced Si-photodetector (ThorLabs PDA155) in a configuration that replicated that used in the photoreactor. In this system, the output optical power was controlled using a pulse width modulation (PWM) circuit and the RMS current intensity was measured with a multimeter (UniVolt DT-64). The disinfection experiments were carried out with a RMS current intensity of 240 mA, corresponding to a UV irradiance of 23 W/m^2 and a photon flux of 5.53×10^{-7} E/s.

The PMS/UV-A LED and PMS/M^{n+}/UV-A LED experiments were carried out using 0.1 mM as an optimal dosage of PMS and transition metals [Fe^{2+} and Co^{2+}] in bacteria inactivation (Rodríguez-Chueca et al., 2017). However, the optimal dosage for removing *C. albicans* was 5 mM for PMS and 2.5 mM for transition metals.

2.3. Analytical determination

Chemical oxygen demand (COD) was measured according to Method 410.4 of the US EPA (EPA, 1993), using a HACH DR/2400 portable spectrophotometer. The pH and the reduction potential were determined by a HANNA pH 209 laboratory meter following Standard Method 4500-H^+-B and 2580 (Eaton et al., 2005), respectively. Conductivity was measured using a Crison Basic as indicated in ISO 7888, 1985. Turbidity was measured according to ISO 7027, 1999 using a HACH 2100 IS Turbidimeter and the Total Suspended Solids (TSS) were measured by spectrophotometry according to Standard Method 2540D (Eaton et al., 2005) using a HACH DR/2400 portable spectrophotometer.

E. coli, *B. mycoides*, *S. aureus* and *C. albicans* concentrations were determined by the spread plate method (Standard Method 9215C; Eaton et al., 2005) after a serial 10-fold dilution in sterilized saline solution (NaCl 0.9%). Aliquots of diluted samples were plated on Chromocult agar (Merck) for *E. coli* and LB agar for *B. mycoides* and *S. aureus*. YMA was used to quantify *C. albicans*. Colonies were counted after 24 h of incubation at 37 °C. The microorganism detection limit (DL) was 1 CFU/mL. Microbial regrowth was estimated after the sample storage at room temperature for 24 and 48 h, after the sampling time, *t*. *B. mycoides* endospores were stained using the differential staining (Schaeffer and Fulton, 1933). Briefly, bacterial suspensions were fixed by heat and stained with malachite green (6 min), and after cooling the slide, washed with tap water and stained with safranin (30 s). This procedure stained in green and in red the endospores and vegetative or mother cells, respectively. Endospores were observed under a Nikon Eclipse E600 light microscope, at 1000× magnification.

2.4. Kinetic modeling

Mathematical inactivation models applied to describe the microorganism inactivation kinetics (Table 1) were fitted using Microsoft® Excel: Solver and GInaFiT (Geeraerd and Van Impe Inactivation Fitting Tool) (Geeraerd et al., 2005).

3. Results and discussion

3.1. Bacteria inactivation

3.1.1. PMS/UV-A LED treatments

Fig. 1 shows the inactivation of bacteria with the PMS/UV-A LED process (*E. coli* Fig. 1a; *B. mycoides* Fig. 1b; *S. aureus* Fig. 1c). The highest rate of microbial inactivation (4.81–7.28 log after 90 min,

Table 1
Mathematical kinetic models fitted to microbial populations after different disinfection approaches. Log linear (L); Log linear with shoulder (LS); Log linear with tail (LT); Log linear with shoulder and tail (LST); Hom (H); Weibull (W); Weibull with tail (WT); Double Weibull (DW); Biphasic (B); Biphasic with shoulder (BS).

Kinetic model	Equation	Parameters	Reference
L	$N = N_0 \cdot e^{-k \cdot t}$	k	Bigelow and Esty, 1920
LS	$N = N_0 \cdot e^{-k \cdot t} \cdot \frac{e^{k \cdot Sl}}{(1+(e^{k \cdot Sl}-1) \cdot e^{-k \cdot t})}$	k, Sl	Geeraerd et al., 2000
LT	$N = (N_0 - N_{res}) \cdot e^{-k \cdot t} + N_{res}$	k, N_{res}	Geeraerd et al., 2000
LST	$N = (N_0 - N_{res}) \cdot \frac{e^{-k \cdot t} \cdot e^{k \cdot Sl}}{(1+e^{k \cdot Sl}-1) \cdot e^{-k \cdot t}} + N_{res}$	k, N_{res}, Sl	Geeraerd et al., 2000
H	$Log\frac{N_t}{N_0} = -k \cdot C^n \cdot t^m = -K \cdot t^m$	k, n, m	Hom, 1972
W	$Log\frac{N_t}{N_0} = -\left(\frac{t}{\delta}\right)^p$	δ, p	Mafart et al., 2002
WT	$N = (N_0 - N_{res}) \cdot 10^{-\left(\frac{t}{\delta}\right)^p} + N_{res}$	δ, p, N_{res}	Albert and Mafart, 2005
DW	$N(t) = \frac{N_0}{1+10^{\alpha}}\left[10^{-\left(\frac{t}{\delta_1}\right)^{p_1+\alpha}} + 10^{-\left(\frac{t}{\delta_2}\right)^{p_2}}\right]$	δ_1, δ_2, p_1, p_2, α	Coroller et al., 2006
B	$Log\frac{N_t}{N_0} = Log[P \cdot e^{-k_1 \cdot t} + (1-P) \cdot e^{-k_2 \cdot t}]$	P, k_1, k_2	Cerf, 1977
BS	$Log\frac{N_t}{N_0} = Log\left[f \cdot e^{-k_1 \cdot t} \cdot \frac{e^{k_1 \cdot S_1}}{1+(e^{k_1 \cdot S_1}-1) \cdot e^{-k_1 \cdot t}} + (1-f) \cdot e^{-k_2 \cdot t} \cdot \left(\frac{e^{k_1 \cdot S_1}}{1+(e^{k_1 \cdot S_1}-1) \cdot e^{-k_1 \cdot t}}\right)^{\frac{k_1}{k_2}}\right]$	P, k_1, k_2, Sl	Geeraerd et al., 2005, 2006

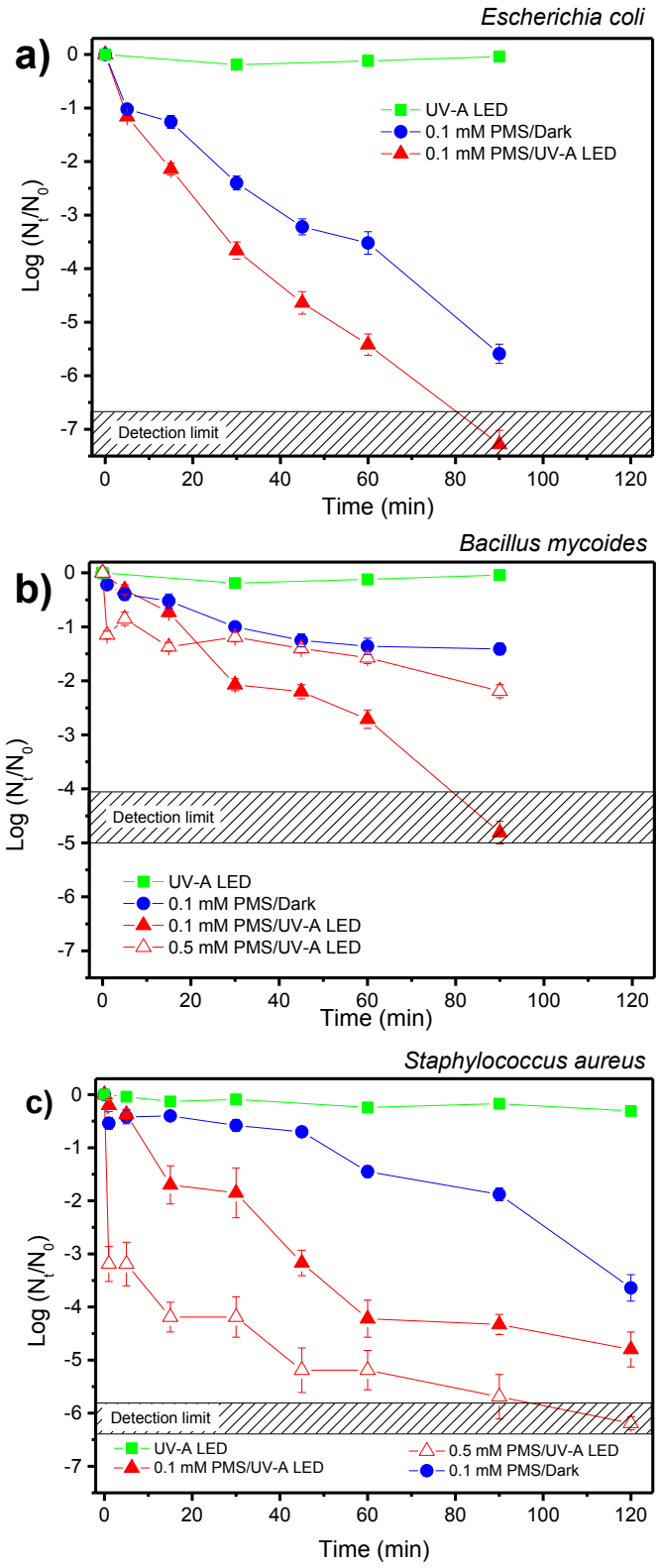

Fig. 1. Inactivation of (a) *E. coli*; (b) *B. mycoides* and (c) *S. aureus* through the treatments PMS/UV-A LED.

depending on the bacteria) was achieved using PMS in the range 0.1–0.5 mM and with UV-A LED irradiation. Higher PMS concentrations up to 10 mM yielded lower inactivation rates (data not shown). The application of PMS in dark (PMS/Dark) brought about a considerable reduction of the *E. coli* population (5.59 log in 90 min) but the bacteria inactivation with UV-A LED radiation alone was negligible (<0.50 log). *B. mycoides* cells (Fig. 1b) were more resilient than *E. coli* (Fig. 1a) at equal PMS concentration. Increasing the PMS concentration from 0.1 to 0.5 mM resulted in a faster inactivation of *B. mycoides,* however, the rapid rate observed during the first minute was followed by a significant reduction of the inactivation rate (2.19 log after 90 min) due to the formation of endospores which exhibit stronger resistance to oxidation. The endosporogenesis was observed and confirmed, after staining under microscope (Schaeffer and Fulton, 1933) for the samples collected during the first 10 min of contact time. In *B subtilis*, the formation of asymmetric division and forespore with its septa has been observed after 15 min (Ojkic et al., 2016) and the release of mature endospores may occur 90 min after the initial formation of endospores (Serrano et al., 2011).

Finally, the results for *S. aureus* (Fig. 1c) demonstrated also the effectiveness of the PMS/UV-A LED process in comparison to PMS/Dark and UV-A LED alone. The inactivation rate with (0.1 mM PMS) was similar to that observed on *B. mycoides*, however, in contrast the rate observed at higher PMS concentration (0.5 mM) was higher than that observed with 0.1 mM.

The kinetic parameters (k and δ) obtained after the fitting of eight different mathematical bacteria inactivation models on the results obtained with the PMS/UV-A LED and PMS/Dark processes, are presented in Table 2. The Hom model (H) fitted the inactivation results for all bacteria. The Hom's kinetic rate constants for the PMS/UV-A LED inactivation of the bacteria were as follows: *E. coli* (0.39 min^{-1}) > *S. aureus* (0.33 min^{-1}) > *B. mycoides* (0.06 min^{-1}) and in the absence of radiation (PMS/Dark) were *S. aureus*: *E. coli* (0.18 min^{-1}) > *B. mycoides* (0.15 min^{-1}) > *S. aureus* (0.003 min^{-1}). In addition, Biphasic and Biphasic with Shoulder models satisfactorily fitted the inactivation results obtained for *E. coli* and *S. aureus* populations. These models, as well as the Double Weibull model, are based on the hypothesis that bacterial population is divided into two subgroups, which differ in their resistance to the treatments.

In general, the application of PMS as an alternative method for microorganism inactivation and water disinfection has been rarely reported in the literature. PMS treatment of groundwater contaminated with *E. coli* and *Enterococcus* sp. yielded more than 3 log inactivation after 15 min of exposure time, using 4 mg/L of PMS (6.50 μM) (Bailey et al., 2011). Although *Enterococcus* is also a Gram-positive like *B. mycoides*, higher concentrations of PMS are needed to inactivate more resilient Gram-positive such as the sporulated bacteria.

3.1.2. PMS/M^{n+}/UV-A LED treatments

Fig. 2 shows the bacterial inactivation through the catalytic activation of 0.1 mM PMS without or with UV-A LED/M^{n+}. The activation of PMS UV-A LED by a transition metal [Fe^{2+} or Co^{2}] increased the inactivation rate of *E. coli* (Fig. 2a): the combination of PMS with Fe^{2+} reached 2.60 log during the first minute of treatment, and the detection limit (6.68 log) after 45 min of treatment. The results obtained were similar to those observed with Co^{2+} as PMS activator. An identical pattern was observed for *B. mycoides* during the first few minutes of treatment with PMS/M^{n+}/UV-A LED (Fig. 2b). Nevertheless, after 30 min (2.30 and 3.04 log with Co^{2+} and Fe^{2+}, respectively) the inactivation yield stabilized and in contrast to the treatment with PMS/UV-A LED, it reached the detection limit (DL) at a longer time after 120 min, Therefore, the highest inactivation values obtained were 3.22 and 3.42 log with Co^{2+} and Fe^{2+} respectively.

Finally, the inactivation behaviour of *S. aureus* followed a different behaviour (Fig. 2c). The combination PMS with Co^{2+}/UV-A

Table 2
Kinetic fitting parameters of *E. coli*, *B. mycoides* and *S. aureus* inactivation after PMS/UV-A LED treatments.

Kinetic model	*E. coli*			*B. mycoides*			*S. aureus*		
	k_1 (min^{-1})/δ_1 (min)	k_2 (min^{-1})/δ_2 (min)	R^2/RMSD	k_1 (min^{-1})/δ_1 (min)	k_2 (min^{-1})/δ_2 (min)	R^2/RMSD	k_1 (min^{-1})/δ_1 (min)	k_2 (min^{-1})/δ_2 (min)	R^2/RMSD
0.1 mM PMS/UV-A LED									
L (k)	0.18	–	0.97/0.51	0.12	–	0.97/0.30	0.10	–	0.88/0.69
H (k)	0.39	–	0.99/0.09	0.06		0.97/0.26	0.33	–	0.96/0.37
LT (k)	–	–	–	–	–	–	0.16	–	0.98/0.31
W (δ)	10.00	–	0.98/0.44	19.73	–	0.97/0.34	5.28	–	0.96/0.44
WT (δ)	–	–	–	–	–	–	12.45	–	0.98/0.33
DW (δ)	4.35	6.02	0.99/0.13	17.41	65.87	0.99/0.12	–	–	–
B (k)	0.34	0.14	0.99/0.20	–	–	–	0.16	0.02	0.98/0.32
BS (k)	0.39	0.14	0.99/0.28	–	–	–	0.17	0.02	0.98/0.38
0.1 mM PMS/Dark									
L (k)	0.13	–	0.98/0.32	0.05	–	0.94/0.14	0.06	–	0.89/0.39
H (k)	0.18	–	0.98/0.18	0.15	–	0.98/0.07	0.003	–	0.95/0.29
LS (k)	–	–	–	–	–	–	0.09	–	0.96/0.27
W (δ)	12.10	–	0.98/0.31	34.81	–	0.98/0.09	66.92	–	0.97/0.24
DW (δ)	0.39	21.03	0.99/0.27				–	–	–
B (k)	–	–	–	0.08	0.00	0.98/0.11	–	–	–
BS (k)	–	–	–	0.08	0.00	0.98/0.14	–	–	–

LED considerably increased the inactivation rate of *S. aureus* (6.10 log), compared to the treatment with non-activated PMS/UV-A LED radiation (4.80 log), or the PMS/UV-A LED combined with Fe^{2+} (3.17 log).

In order to increase the microbial inactivation rate and reduce the inactivation time, a second dose of reagents (PMS and the transition metal) was supplemented at the 15th min of treatment (Fig. 3). As observed in Fig. 3a, this second dose did not result in an increase of the inactivation of *E. coli*, and the detection limit was reached almost at the same time as for the treatments carried out with only one addition of reagents. The low resistance of *E. coli* to the oxidative treatments made the second dose of reagents redundant. For *B. mycoides*, the second dose of reagents diminished the inactivation rate. The increase of oxidative stress triggered the sporulation process, increasing the physiological resistance of the *B. mycoides* population (Fig. 3b) and the generation of endospores was confirmed by staining. Finally, Fig. 3c shows the inactivation of *S. aureus*, which dramatically increased with the second dosing of reagents with the combination of PMS with Fe^{2+}. However, such effect was not observed with the combination PMS with Co^{2+} which showed a negligible rate increase. The DL was achieved at 120 min in both cases, i.e. PMS with Fe^{2+} or Co^{2+}. Although authors as Spuhler et al. (2010) reported the *E.coli* inactivation efficiency of Fe(II)/hυ and Fe(III)/hυ systems, this effect has not been observed in this research (data not shown), nor Fe(II) neither Co(II).

Tables 3 and 4 show the kinetic parameters (k and δ) obtained after the fitting of the inactivation results with the PMS/M^{n+}/UV-A LED process with one and two additions of reagents with the different mathematical models. As shown, only the Hom model could fit all the inactivation results. Comparing the values of the Hom model kinetic constants (Tables 2 and 3), the combination of Co^{2+} or Fe^{2+} with PMS and UV-A LED radiation resulted in a significant increase in the inactivation rate of all bacteria. As an exception the PMS/Fe^{2+}/UV-A LED (0.05 min^{-1}) was less effective than the PMS/UV-A LED (0.33 min^{-1}) process for the inactivation of *S. aureus*. This behavioural pattern had already been observed in Fig. 2c. In general, the highest kinetic constants were achieved through the catalytic activation of PMS with Co^{2+}, the exception being the case of *B. mycoides*, where a higher inactivation rate was obtained using Fe^{2+}.

With double dosing of reagents, the DL was attained more quickly. However, the kinetic constants were slightly lower (Table 4) than those obtained with a single dose (Table 3), except for *S. aureus*. For *S. aureus*, a second dose of reagents increased the inactivation rate (k and δ) in almost all models, both with Co^{2+} or Fe^{2+}.

Anipsitakis et al. (2008) reported the use of PMS in combination with traces of Co^{2+} as an *in situ* swimming-pool sanitizer (Anipsitakis et al., 2008). The application of 25 mg/L of PMS and 0.1 mg/L of Co^{2+} was proven efficient, but with a rather slow disinfection rate. Under the pool water conditions, a 4-log kill of *E. coli* was achieved after 60 min of treatment. This result does not meet the requirements as an EPA-registered swimming pool sanitizer, which requires 6-log kill of *E. coli* ATCC 11229, and of *Enterococcus faecium* ATCC 6569, within 30 s. Although still short of the standard required for use as a swimming-pool sanitizer, the results presented in this manuscript show that the application of 0.1/0.1 mM PMS/Co^{2+}/UV-A LED radiation reached almost 3 log inactivation of *E. coli* after just 1 min of treatment, therefore such process could potentially be used in a combined water disinfection process.

The mechanism of attack of the sulphate radical on bacteria is still unknown. However it has been hypothesized that the increase of oxidative conditions around the bacteria cells involves overstress conditions that results in their inactivation. Understanding the process is made difficult by the necessity to take into account the large number of exogenous agents able to attack bacteria, such as sulphate and hydroxyl radicals, UV-A radiation, and the transition metals [Fe^{2+} and Co^{2+}]. Fig. 4 is an adaptation from the research of Ma et al. (2009) and Spuhler et al. (2010), showing the possible pathways in the inactivation of *E. coli* (Gram-negative bacteria) using PMS/UV-A LED and PMS/M^{n+}/UV-A LED treatments. Taking into account each oxidative agent individually, there are a variety of possible oxidative effects on the cell. For instance, UV-A light can damage catalase (CAT) and superoxide dismutase (SOD) enzymes, which are responsible for the elimination of metabolic generated H_2O_2 and $O_2^{\bullet-}$, so their dysfunctioning could increase the intracellular concentration of these ROS species (Imlay, 2008). Furthermore, endogenous and exogenous photosensitizers (PS) can absorb UV-A radiation, reach an excited state and attack biomolecules or react with oxygen generating ROS species (Acra et al., 1990; Reed, 2004) causing oxidative damage to the bacteria. In addition, UV-A radiation can damage iron containing proteins like Ferritin, leading to the intracellular release of Fe^{2+} which enhanced

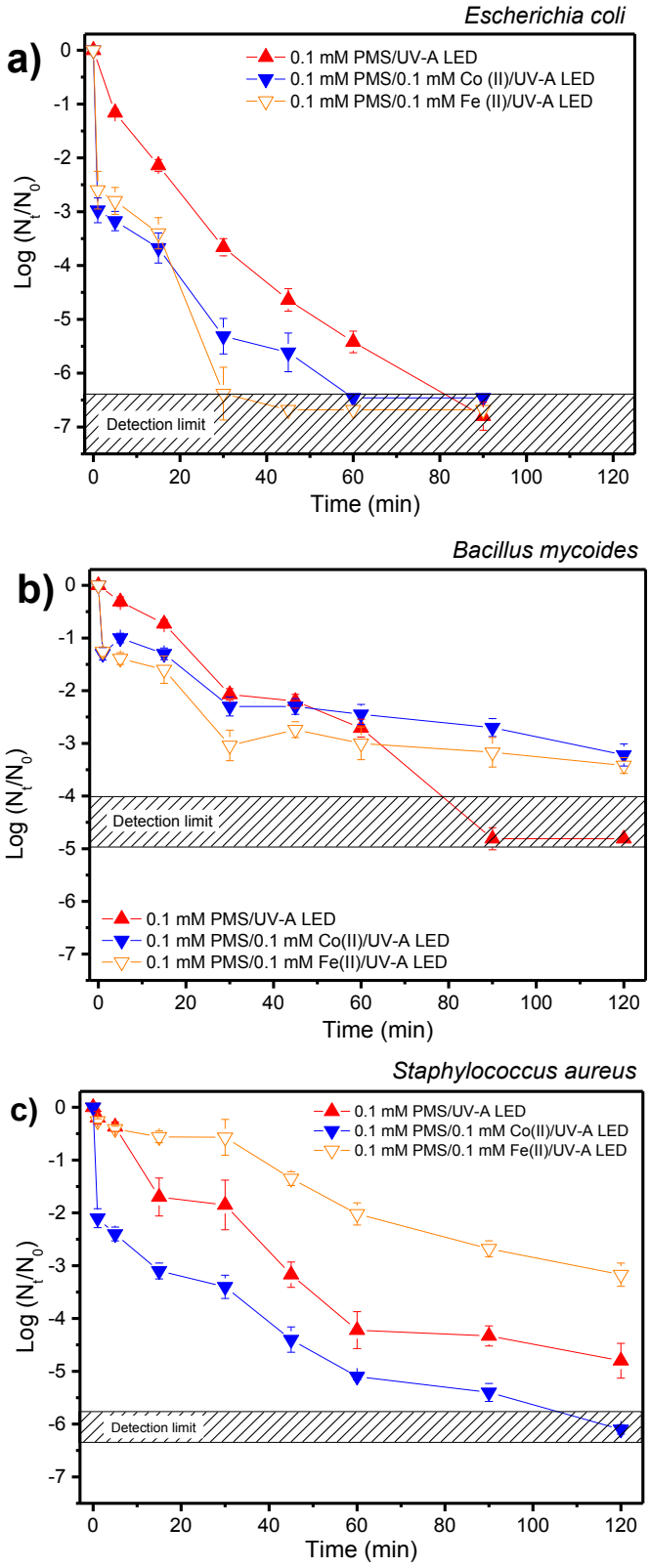

Fig. 2. Inactivation of (a) *E. coli*; (b) *B. mycoides* and (c) *S. aureus* after a single treatments PMS/M^{n+}/UV-A LED [M^{n+} = Fe^{2+} or Co^{2+}].

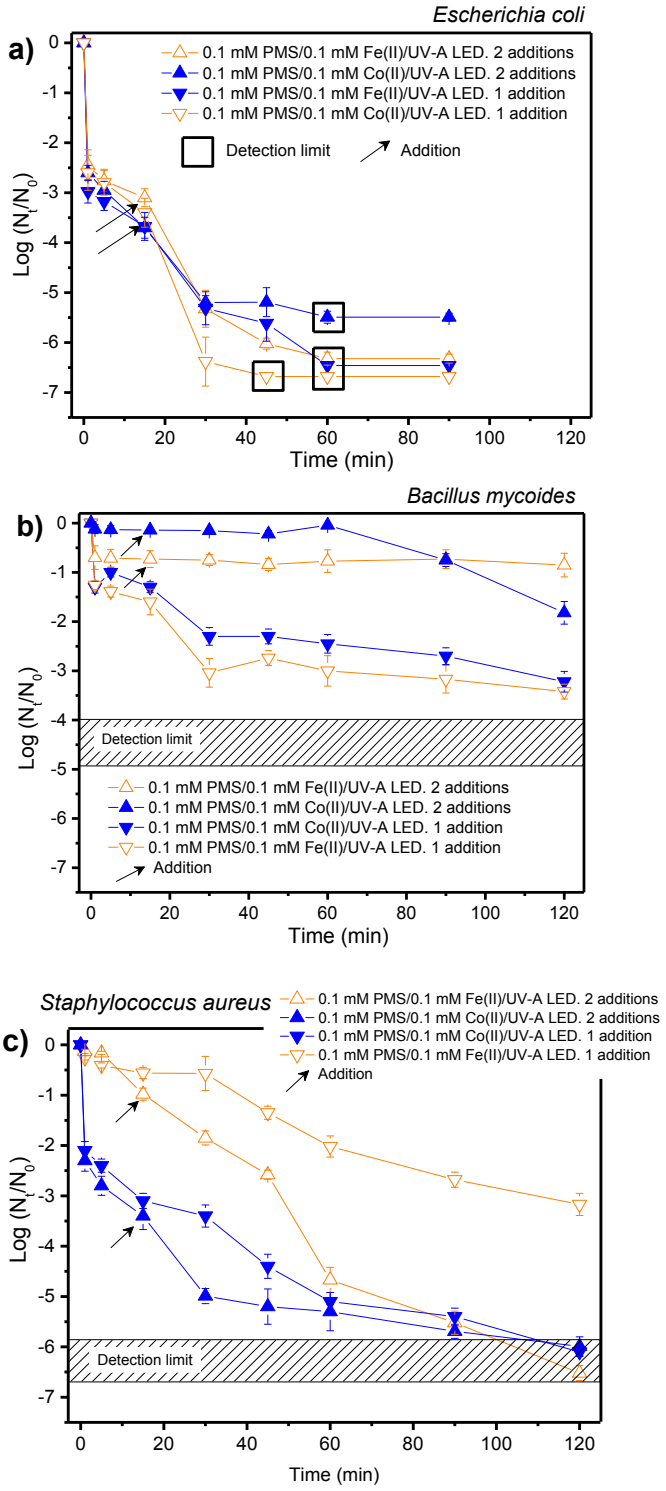

Fig. 3. Inactivation of (a) *E. coli*; (b) *B. mycoides* and (c) *S. aureus* through the treatments PMS/M^{n+}/UV-A LED [M^{n+} = Fe^{2+} or Co^{2+}] with two reagent's additions.

free iron pools that will scavenge the heme and iron released by subsequent oxidising (UV-A) treatments (Hoerter et al., 1996; Tyrrell et al., 2000).

While UV-A radiation causes oxidative stress to the cell, other agents, such as the transition metals, such as Fe, Co, Ni, Cu, etc. can also provoke significant damage. Although some transition metals are essential oligonutrients satisfying important biological functions of microorganisms, an excess of them can be lethal (Blaha et al., 2011). The membranes of bacteria are formed by different proteins whose functions are related to the selective transport of

Table 3
Kinetic fitting parameters of *E. coli*, *B. mycoides* and *S. aureus* inactivation after PMS/M^{n+}/UV-A LED treatments.

Kinetic model	*E. coli*			*B. mycoides*			*S. aureus*		
	k_1 (min^{-1})/δ_1 (min)	k_2 (min^{-1})/δ_2 (min)	R^2/RMSD	k_1 (min^{-1})/δ_1 (min)	k_2 (min^{-1})/δ_2 (min)	R^2/RMSD	k_1 (min^{-1})/δ_1 (min)	k_2 (min^{-1})/δ_2 (min)	R^2/RMSD
0.1 mM PMS/0.1 mM Fe(II)/UV-A LED									
L (k)	–	–	–	–	–	–	0.06	–	0.97/0.21
H (k)	2.12	–	0.93/0.65	1.06	–	0.98/0.07	0.05	–	0.97/0.19
LST (k)	–	–	–	–	–	–	0.09	–	0.98/0.19
W (δ)	0.07	–	0.93/0.82	–	–	–	35.50	–	0.97/0.23
WT (δ)	–	–	–	–	–	–	40.34	–	0.98/0.20
DW (δ)	–	–	–	–	–	–	42.93	116.86	0.99/0.17
B (k)	0.39	0.002	0.92/0.95	0.21	0.01	0.90/0.45	–	–	–
BS (k)	–	–	–	–	–	–	0.14	0.03	0.99/0.19
0.1 mM PMS/0.1 mM Co(II)/UV-A LED									
H (k)	2.39	–	0.97/0.38	0.80	–	0.93/0.25	1.54	–	0.97/0.30
LT (k)	–	–	–	–	–	–	0.15	–	0.88/0.76
W (δ)				3.33	–	0.93/0.31	0.32	–	0.97/0.36
B (k)	7.21	0.09	0.95/0.67	0.16	0.02	0.90/0.42	5.16	0.07	0.97/0.38

Table 4
Kinetic fitting parameters of *E. coli*, *B. mycoides* and *S. aureus* inactivation after PMS/M^{n+}/UV-A LED treatments with two different additions of reagents.

Kinetic model	*E. coli*			*B. mycoides*			*S. aureus*		
	k_1 (min^{-1})/δ_1 (min)	k_2 (min^{-1})/δ_2 (min)	R^2/RMSD	k_1 (min^{-1})/δ_1 (min)	k_2 (min^{-1})/δ_2 (min)	R^2/RMSD	k_1 (min^{-1})/δ_1 (min)	k_2 (min^{-1})/δ_2 (min)	R^2/RMSD
0.1 mM PMS/0.1 mM Fe(II)/UV-A LED [2 additions]									
L (k)	–	–	–	–	–	–	0.13	–	0.97/0.48
H (k)	1.92	–	0.95/0.49	0.68	–	0.98/0.04	0.11	–	0.98/0.37
LT (k)	0.31	–	0.91/0.83	–	–	–	0.15	–	0.98/0.37
LST (k)	–	–	–	–	–	–	0.16	–	0.98/0.40
W (δ)	–	–	–	–	–	–	15.17	–	0.97/0.49
WT (δ)	–	–	–	–	–	–	21.18	–	0.98/0.40
DW (δ)	–	–	–	–	–	–	21.94	66.89	0.99/0.28
B (k)	0.31	0.01	0.91/0.92	–	–	–	0.16	0.06	0.99/0.36
BS (k)	–	–	–	–	–	–	0.17	0.06	0.99/0.39
0.1 mM PMS/0.1 mM Co(II)/UV-A LED [2 additions]									
H (k)	2.38	–	0.97/0.30	$1.37 \cdot 10^{-5}$	–	0.95/0.13	2.12	–	0.98/0.26
LS (k)	–	–	–	0.09	–	0.98/0.09	–	–	–
W (δ)	0.01	–	0.97/0.38	3.80	–	0.98/0.10	–	–	–
WT (δ)	1.24	–	0.90/0.79	–	–	–	–	–	–
DW (δ)	–	–	–	0.98	105.88	0.97/0.12	–	–	–
B (k)	6.11	0.07	0.93/0.67	–	–	–	1.04	0.05	0.91/0.77
BS (k)	–	–	–	–	–	–	–	–	–

molecules into the cytosol. The location of the periplasmic space differentiates Gram-negative from Gram-positive bacteria, which in the former is located between the outer and the inner membranes. In consequence, in Gram-negative bacteria the, metals have to diffuse through the periplasm before entering the cytosol. The porins, trimeric proteins embedded in the outer membrane (OM), allow the passive diffusion of metal ions across the OM (Fig. 4). In order to meet cellular metal demands, however, the cytosol must effectively concentrate metal ions. Consequently, there are high-affinity active transport systems in both membranes (outer and inner) and in the plasma, the purpose of which is to transport and release metal ions into the cytosol (Ma et al., 2009). Any excess concentration of Fe^{2+} or Co^{2+}, resulting from the PMS/M^{n+}/UV-A LED treatments, may increase the mortality of the bacteria. Usually bacteria deploy detoxification mechanisms to remove excess metals. In *E. coli*, RcnA is an efflux pump responsible for both Ni and Co detoxification, whilst the Cation Diffusion Facilitator (CDF) is responsible for Fe. RcnA confers resistance to Ni and Co, and its expression is induced by these two metals and not by other divalent cations (Rodrigue et al., 2005). So, it could be hypothesised that defective operation of these pumps as a consequence of Co^{2+} or Fe^{2+} excess may contribute to bacteria inactivation. Another hypothesis related to Fe^{2+} is based on the diffusion of extracellular Fe^{2+} into the cytoplasm and the subsequent reaction with intracellular H_2O_2 via a Haber-Weiss reaction, generating hydroxyl radicals that directly attack cellular DNA.

Perhaps the most important contribution to the cellular attack is provided by sulphate and hydroxyl radicals generated in the PMS/UV-A LED and PMS/M^{n+}/UV-A LED processes. The literature regarding the use of sulphate radicals in microbial inactivation is still scarce and an understanding of their attack mechanism is based on the surmise that their behaviour may be similar to that exerted by hydroxyl radicals. Sulphate and hydroxyl radicals react with the cellular constituents responsible for lipid peroxidation in intracellular and cellular membranes, enhancing permeability and inactivation (Spuhler et al., 2010; Reed, 2004; Cabiscol et al., 2000). It is also well-known that hydroxyl radicals are the only ROS which can directly damage DNA (Sattler et al., 2000), and there are no reports on the action of sulphate radicals on DNA.

Although the majority of the literature reports the oxidative stress on *E. coli* (Gram-negative bacteria), the relevant mechanisms could be quite similar for other bacteria, even for Gram-positive bacteria, and consequently oxidative stress could influence them in a similar way. There are important structural differences

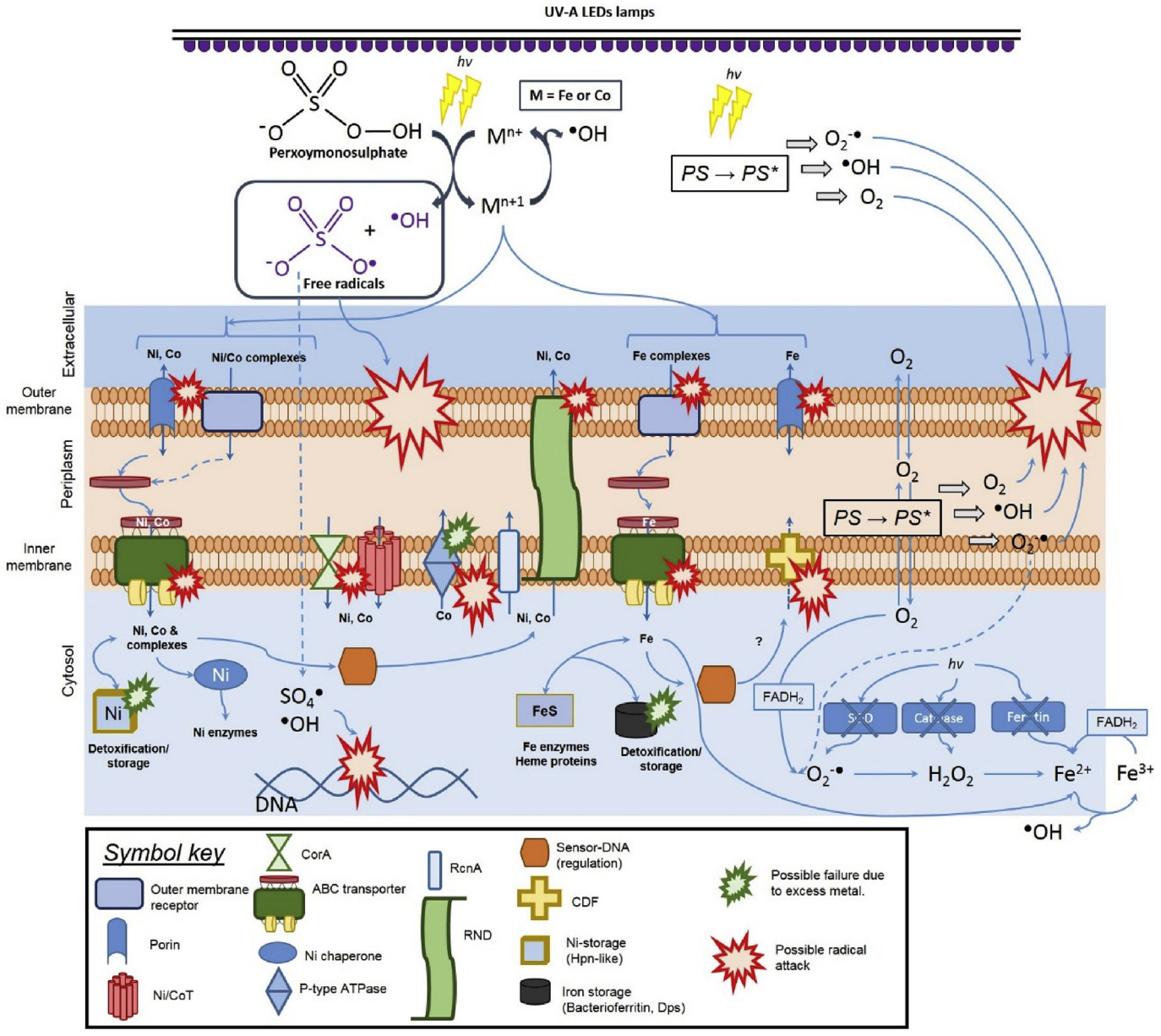

Fig. 4. Possible routes involved in photo-inactivation of *E. coli* (Gram-negative bacteria) through PMS/UV-A LED and PMS/M^{n+}/UV-A LED (Adapted from Ma et al., 2009; Spuhler et al., 2010).

between both types of bacteria, and these are shown in Fig. 5. As a result of these differences, Gram-positive bacteria are generally more resistant than Gram-negative bacteria (Madigan et al., 2012). However, both types of bacteria could also possess similar efflux pumps, the aim of which is to maintain homeostasis in the cytoplasm, and thus share the same vulnerability to pump disruption. Finally, the hypothesis that both sulphate and hydroxyl radicals lethally attack the bacteria cell membranes and DNA and prevent their re-growth is proposed.

3.2. *Candida albicans* inactivation

Fig. 6 shows the inactivation of the fungus *C. albicans* using the PMS/UV-A LED (Fig. 6a) and PMS/M^{n+}/UV-A LED (Fig. 6b) processes. Lower concentrations of PMS (0.1 and 0.5 mM) were ineffective on the inactivation of *C. albicans*, while a tenfold increase (5 mM) resulted in a significant reduction of *C. albicans* (Fig. 6a). Under these operational conditions, combined with UV-A LED, the DL was reached at 120 min (5.61 log).

The inactivation rate of this species was drastically improved using a combination of PMS with a transition metal (Fe^{2+} or Co^{2+}), especially with Co^{2+}. As shown in Fig. 6b, after 15 min of contact time 2 log inactivation was achieved with the combination of 5 mM of PMS with 2.5 mM of Fe^{2+}. When Co^{2+} was used as a metal catalyst for PMS, 4.30 log inactivation was observed during the first minute of contact time, and the DL was reached after 30 min (5.30 log). The fast inactivation observed with PMS and Co^{2+} did not warrant further doses of reagents. However, a second dose of PMS and Fe^{2+} supplemented after the 15th minute (Fig. 6b) produced a more rapid rate of inactivation to the DL (after 30 min, 5.64 log).

Table 5 shows the kinetic parameters (k and δ) obtained after fitting the mathematical models to the inactivation results of

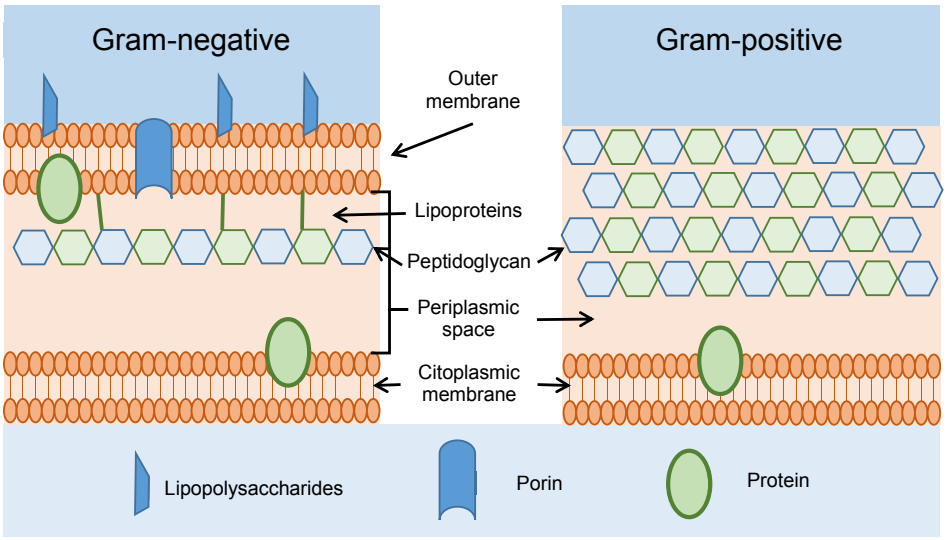

Fig. 5. Structural differences between Gram-negative and Gram-positive bacteria.

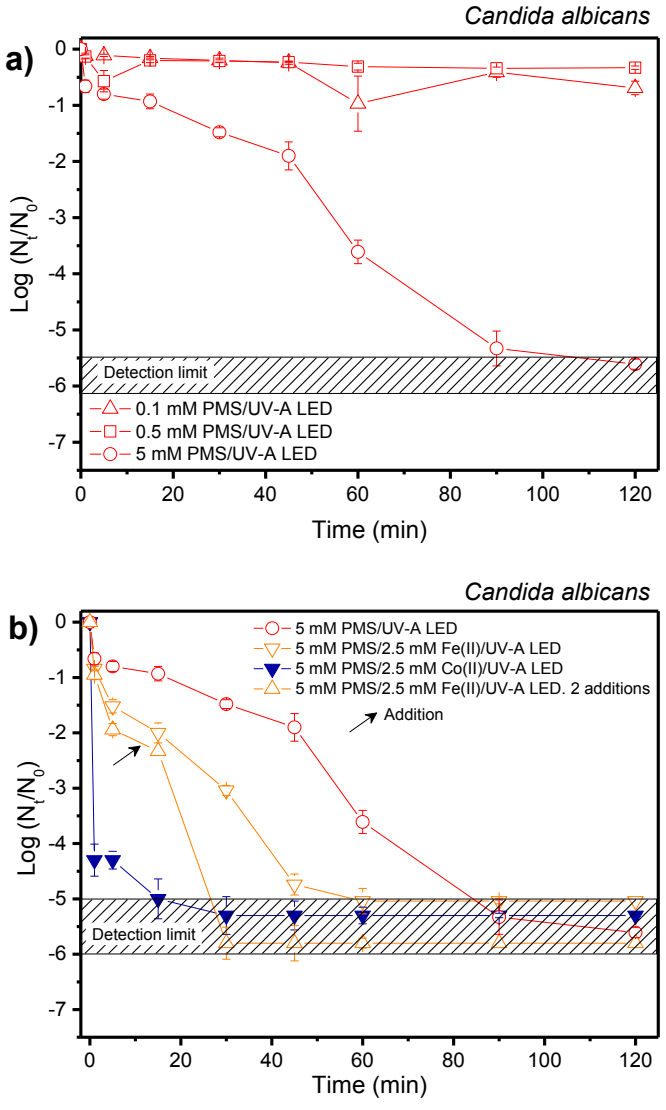

Fig. 6. Inactivation of *C. albicans* through the treatments (a) PMS/UV-A LED; (b) PMS/M^{n+}/UV-A LED [M^{n+} = Fe^{2+} or Co^{2+}].

Table 5
Kinetic fitting parameters of *C. albicans* inactivation after PMS/UV-A LED and PMS/M^{n+}/UV-A LED treatments.

Kinetic model	*C. albicans*		
	k_1 (min^{-1})/δ_1 (min)	k_2 (min^{-1})/δ_2 (min)	R^2/RMSD
5 mM PMS/UV-A LED			
L (k)	0.11	–	0.96/0.47
H (k)	0.09	–	0.95/0.44
LS (k)	0.11	–	0.96/0.50
W (δ)	20.19	–	0.96/0.51
WT (δ)	32.87	–	0.98/0.34
B (k)	0.12	$3.48 \cdot 10^{-3}$	0.97/0.48
5 mM PMS/2.5 mM Fe (II)/UV-A LED			
H (k)	0.90	–	0.94/0.47
B (k)	0.21	0.00	0.98/0.14
BS (k)	0.21	0.00	0.98/0.18
5 mM PMS/2.5 mM Co (II)/UV-A LED			
H (k)	4.23	–	0.99/0.15
LT (k)	10.07	–	0.96/0.38
5 mM PMS/2.5 mM Fe (II)/UV-A LED (2 additions)			
H (k)	1.46	–	0.88/0.77
B (k)	0.37	0.00	0.97/0.54

C. albicans obtained with the PMS/UV-A LED and PMS/M^{n+}/UV-A LED processes, with either one or two reagents doses. As previously observed in the kinetic parameters of bacteria, the Hom model fitted the inactivation results of *C. albicans* (Table 5). The inactivation rate of *C. albicans* increased 10-fold with the addition of Fe^{2+} (0.90 min^{-1}) and 40-fold with the addition of Co^{2+} (4.23 min^{-1}) in combination with PMS, in comparison to the results obtained with the PMS/UV-A LED process (0.09 min^{-1}). A further dose of PMS and Fe^{2+} increased the inactivation rate of *C. albicans*, (1.46 min^{-1}).

Kühn et al. (2003) reported that *C. albicans* was more resilient, when compared to other microorganisms such as *E. coli*, *Pseudomonas aeruginosa*, *S. aureus* and *Enterococcus faecium*, when treated with TiO_2/UV photocatalysis. Although *C. albicans* is a commensal constituent of normal gut flora, this fungus can be pathogenic and can developed defence mechanisms against the immune cells of the host, resisting the high oxidative stress caused by these cells (Jiménez-López and Lorenz, 2013). Studies of the interaction model of *C. albicans* versus macrophages, have shown that the fungus is resistant to stress caused by ROS and nitrogen reactive species (RNS) generated by macrophages. *C. albicans* encode a catalase

(cat1), and six superoxide dismutases (SOD), with three of them extracellular (Sod4-6) and are able to detoxify the ROS released by macrophages (Frohner et al., 2009). Defences against intracellular RNS are in the form of three flavohemoglobins enzymes (Ullmann et al., 2004). Therefore, it is possible to hypothesize that the natural resistance of *C. albicans* to macrophages may induce a higher resilience than bacteria to sulphate radicals (SOS). Metal toxicity in *Saccharomyces cerevisiae* are involved in ROS generation, lipid peroxidation, and depletion of glutathione (GSH), a major antioxidant in eukaryotic cells. Yeast seems to use the same mechanisms to resist either iron or cobalt stress (Wang et al., 2017; Stadler and Schweyen, 2002). In the first line of defence, yeasts increased cobalt sequestration in the vacuole and later increased the expression of genes involved in the oxidative stress (Stadler and Schweyen, 2002; Conklin et al., 1992; Pimentel et al., 2014). More recently, Wang et al. (2017), reported that *S. cerevisiae* yeast cells treated with Cd^{2+} also increased intracellular Ca^{2+} levels and provoked the collapse of the mitochondrial membrane potential. Cobalt also significantly inhibited *C. albicans* clamidospore germination when compared to other metals such as iron and zinc (Hazen and Cutler, 1983). These responses may explain the combined effect of PMS and metal (either Fe^{2+} or Co^{2+}), which was reflected by a 10-fold and 40-fold increase, respectively, on the inactivation rate of *C. albicans*.

4. Conclusions

This study presents an alternative approach for the disinfection of surface freshwater through the combined use of PMS/UV-A LED with or without M^{n+}. These stressors were tested on four microbial species, which varied in their ultra-structure and natural resistance mechanisms including the cell wall structure, endospore production and oxidative enzymes. The main conclusions that can be drawn from this study are:

- The photolytic activation of PMS through UV-A LED radiation achieves complete inactivation of the bacteria *E. coli*, *B. mycoides* and *S. aureus* using low dosages of PMS (0.1 mM) and at circumneutral pH. However, higher dosages of PMS (5 mM) are necessary to inactivate *C. albicans* due to its higher oxidative stress resistance.
- The inactivation rate of microorganisms can be increased during the first few minutes of contact time by the catalytic activation of PMS using a transition metal [Fe^{2+} or Co^{2+}]. However, the rapid catalytic consumption of sulphate radicals results in a lack of oxidant at later stages of the disinfection process and further dosing of PMS may be required.
- The combination of PMS with Co^{2+} obtained higher inactivation values for *S. aureus* and *C. albicans* than its combination with Fe^{2+}, which may be related to the fact that cobalt is more toxic than iron to eukaryotic cells.
- The gram-negative bacteria *E. coli* was more sensitive to the disinfection process than the gram-positive counterparts (*B. mycoides* and *S. aureus*) and the fungus *C. albicans*. Therefore, the use of *E. coli* as an indicator or model species for water disinfection studies, should be reconsidered because an efficient inactivation of *E. coli* does not necessarily imply an efficient inactivation of other pathogens.
- The oxidative stress generated through the complexity of PMS/M^{n+}/UV-A LED treatments triggered the formation of endospores in *B. mycoides*. Consequently, more demanding operational conditions may be required to reach the total inactivation of sporulated bacterial species.
- The Hom model satisfactorily fitted the inactivation results of all of the studied microorganisms. In addition, mathematical models based on Weibull distributions and Biphasic and Biphasic with Shoulder models accurately describe the inactivation curve of microorganisms in some of the studied treatments. These models are based on the hypothesis that the bacteria populations have sub-groups with different resilience to the treatments proposed.
- Finally, the use of UV-A LED radiation in treatment processes represent an attractive alternative to the use of conventional UV lamps, since LED are eco-friendly, present low operating cost and have a high-energy efficiency.

Acknowledgments

The authors are grateful to European Investment Funds by FEDER/COMPETE/POCI (POCI-01-0145-FEDER-006958) and National Funds by FCT under the projects UID/AGR/04033/2013 and UID/QUI/00616/2013. Project INNOFOOD - INNOvation in the FOOD sector through the valorization of food and agro-food by-products - NORTE-07-0124-FEDER-0000029, Project INTERACT – Integrative Research in Environment, Agro-Chains and Technology - NORTE-01-0145-FEDER-000017 and Project INNOVINE & WINE - Innovation Platform of Vine and Wine - NORTE-01-0145-FEDER-000038. Jorge Rodríguez-Chueca also acknowledges the funding provided by the Spanish Ministry of Economy and Competitiveness (MINECO) through the Juan de la Cierva-formación grant (No FJCI-2014-20195). Marco S. Lucas also acknowledges the funding provided by the European Union's Horizon 2020 research and innovation programme under the Marie Sklodowska-Curie grant agreement No 660969.

References

Acra, A., Jurdi, M., Mu'allem, H., Karahagopian, Y., Raffoul, Z., 1990. Water Disinfection by Solar Radiation: Assessment and Application. International Development Research Centre (IDRC – Canada), PO Box 8500, Ottawa, Ont., Canada K1G 3H9.

Albert, I., Mafart, P., 2005. A modified Weibull model for bacterial inactivation. Int. J. Food Microbiol. 100, 197–211.

Anipsitakis, G.P., Dionysiou, D.D., 2003. Degradation of organic contaminants in water with sulfate radicals generated by the conjunction of peroxymonosulfate with cobalt. Environ. Sci. Technol. 37, 4790–4797.

Anipsitakis, G.P., Tufano, T.P., Dionysiou, D.D., 2008. Chemical and microbial decontamination of pool water using activated potassium peroxymonosulfate. Water Res. 42, 2899–2910.

Bailey, M.M., Cooper, W.J., Grant, S.B., 2011. , In situ disinfection of sewage contaminated shallow groundwater: a feasibility study. Water Res. 45, 5641–5653.

Bandala, E.R., Peláez, M.A., Dionysiou, D.D., Gelover, S., Garcia, J., Macías, D., 2007. Degradation of 2,4-dichlorophenoxyacetic acid (2,4-D) using cobaltperoximonosulfate in Fenton-like process. Photochem. Photobiol. A 186, 357–363.

Bigelow, W.D., Esty, J.R., 1920. The thermal death point in relation to typical thermophilic organisms. J. Infect. Dis. 27, 602.

Blaha, D., Arous, S., Blériot, C., Dorel, C., Mandrand-Berthelot, M., Rodrigue, A., 2011. The *Escherichia coli* metallo-regulator RcnR represses rcnA and rcnR transcription through binding on a shared operator site: insights into regulatory specificity towards nickel and cobalt. Biochimie 93, 434–439.

Cabiscol, E., Tamarit, J., Ros, J., 2000. Oxidative stress in bacteria and protein damage by reactive oxygen species. Int. Microbiol. 3, 3–8.

Calderone, R.A., 2002. *Candida* and Cadidiasis. ASM Press, USA.

Cerf, O., 1977. A review: tailing of survival curves of bacterial spores. J. Appl. Bacteriol. 42, 1–19.

Conklin, D.S., McMaster, J.A., Culbertson, M.R., Kung, C., 1992. Kung. COT1, a gene involved in cobalt accumulation in *Saccharomyces cerevisiae*. Mol. Cell. Biol. 12, 3678–3688.

Coroller, L., Leguerinel, I., Mettler, E., Savy, N., Mafart, P., 2006. General model, based on two mixed Weibull distributions of bacterial resistance, for describing various shapes of inactivation curves. Appl. Environ. Microbiol. 72, 6493–6502.

Doederer, K., Wolfgang, G., Weinberg, H.S., Farré, M.J., 2014. Factors affecting the formation of disinfection by-products during chlorination and chloramination of secondary effluent for the production of high quality recycled water. Water Res. 48, 218–228.

Douglas, L.J., 1988. *Candida* proteinases and candidiasis. Crit. Rev. Biotechnol. 8, 121–129.

Eaton, A.D., Clesceri, L.S., Rice, E.W., Greenberg, A.E., Franson, M.A.H., 2005. Standard Methods for the Examination of Water and Wastewater, twenty-first ed.

(APA-AWWA-WEF).
Ferro, G., Fiorentino, A., Alferez, M.C., Polo-López, M.I., Rizzo, L., Fernández-Ibáñez, P., 2015. Urban wastewater disinfection for agricultural reuse: effect of solar driven AOPs in the inactivation of a multidrug resistant *E. coli* strain. Appl. Catal. B Environ. 178, 65–73.
Frohner, I.E., Bourgeois, C., Yatsyk, K., Majer, O., Kuchler, K., 2009. *Candida albicans* cell surface superoxide dismutases degrade host-derived reactive oxygen species to escape innate immune surveillance. Mol. Microbiol. 71, 240–252.
Geeraerd, A.H., Herremans, C.H., Van Impe, J.F., 2000. Structural model requirements to describe microbial inactivation during a mild heat treatment. Int. J. Food Microbiol. 59, 185–209.
Geeraerd, A.H., Valdramidis, V.P., Van Impe, J.F., 2005. GInaFiT, a freeware tool to assess non-log-linear microbial survivor curves. Int. J. Food Microbiol. 102, 95–105.
Geeraerd, A.H., Valdramidis, V.P., Van Impe, J.F., 2006. Erratum to "GInaFiT, a freeware tool to assess non-log-linear microbial survivor curves". Int. J. Food Microbiol. 110, 297.
Giannakis, S., Papoutsakis, S., Darakas, E., Escalas-Cañellas, A., Pétrier, C., Pulgarin, C., 2015. Ultrasound enhancement of near-neutral photo-Fenton for effective E. coli inactivation in wastewater. Ultrason. Sonochem 22, 515–526.
Grellier, J., Rushton, L., Briggs, D., Nieuwenhuijsen, M.J., 2015. Assessing the human health impacts of exposure to disinfection by-products–a critical review of concepts and methods. Environ. Int. 78, 61–81.
Hazen, K.C., Cutler, J.E., 1983. Isolation and purification of morphogenic autoregulatory substance produced by *Candida albicans*. J. Biochem. 94, 777–783.
Hoerter, J., Pierce, A., Troupe, C., Epperson, J., Eisenstark, A., 1996. Role of enterobactin and intracellular iron in cell lethality during near-UV irradiation in *Escherichia coli*. Photochem. Photobiol. 64, 537–541.
Hom, L.W., 1972. Kinetics of chlorine disinfection in an ecosystem. J. Sanit. Eng. Div. ASCE 98 (1), 183–193.
Imlay, J.A., 2008. Cellular defenses against superoxide and hydrogen peroxide. Annu. Rev. Biochem. 77 (1), 755–776.
ISO 5667-3, 2012. Water Quality: Sampling - Part 3: Preservation and Handling of Water Samples.
ISO 7027, 1999. Water Quality - Determination of Turbidity.
ISO 7888, 1985. Water Quality - Determination of Electrical Conductivity.
Jiménez-López, C., Lorenz, M.C., 2013. Fungal immune evasion in a model host–pathogen interaction: *Candida albicans* versus macrophages. PLOS Pathog. 9, 1–4.
Kühn, K.P., Chaberny, I.F., Massholder, K., Stickler, M., Benz, V.W., Sonntag, H.G., Erdinger, L., 2003. Disinfection of surfaces by photocatalytic oxidation with titanium dioxide and UVA light. Chemosphere 53, 71–77.
LeChevallier, M.W., Au, K.K., 2004. Water Treatment and Pathogen Control. Process Efficiency in Achieving Safe Drinking Water. World Health Organization, IWA Publishing, London (United Kingdom).
Ma, Z., Jacobsen, F.E., Giedroc, D.P., 2009. Coordination chemistry of bacterial metal transport and sensing. Chem. Rev. 109, 4644–4681.
Madigan, M.T., Martinki, J.M., Dunlap, P.V., Clark, D.P., 2012. Brock: Biology of Microorganisms, thirteenth ed. Pearson Education, San Francisco (USA).
Mafart, P., Couvert, O., Gaillard, S., Legurinel, I., 2002. On calculating sterility in thermal preservation methods: application of the Weibull frequency distribution model. Int. J. Food Microbiol. 72, 107–113.
Ojkic, N., López-Garrido, J., Pogliano, K., Endres, R.G., 2016. Cell-wall remodeling drives engulfment during *Bacillus subtilis* sporulation. Elife 5, e18657.
Parés, R., Juárez, A., 2002. Bioquímica de los microorganismos. Editorial Reverté S.A., Barcelona (Spain).
Pimentel, C., Caetano, S.M., Menezes, R., Figueira, I., Santos, C.N., Ferreira, R.B., Santos, M.A.S., Rodrigues-Pousada, C., 2014. Yap1 mediates tolerance to cobalt toxicity in the yeast *Saccharomyces cerevisiae*. Biochim. Biophys. Acta 1840, 1977–1986.
Reed, R.H., 2004. The inactivation of microbes by sunlight: solar disinfection as a water treatment process. Adv. Appl. Microbiol. 54, 333–365.
Richardson, S.D., Plewa, M.J., Wagner, E.D., Schoeny, R., Demarini, D.M., 2007. Occurrence, genotoxicity, and carcinogenicity of regulated and emerging disinfection by-products in drinking water: a review and roadmap for research. Mutat. Res. 636, 178–242.
Rodrigue, A., Effantin, G., Mandrand-Berthelot, M.A., 2005. Identification of rcnA (yohM), a nickel and cobalt resistance gene in *Escherichia coli*. J. Bacteriol. 187, 2912–2916.
Rodríguez-Chueca, J., Moreira, S.I., Lucas, M.S., Fernandes, J.R., Tavares, P.B., Sampaio, A., Peres, J.A., 2017. Disinfection of simulated and real winery wastewater using sulphate radicals: peroxymonosulphate/transition metal/UV-A LED oxidation. J. Clean. Prod. 149, 805–817.
Rook, J.J., 1974. Formation of haloforms during chlorination of natural water. Water Treat. Exam. 23 (2), 234–243.
Sattler, U., Calsou, P., Boiteux, S., Salles, B., 2000. Detection of oxidative base DNA damage by a new biochemical assay. Arch. Biochem. Biophys. 376, 26–33.
Schaeffer, A.B., Fulton, M.A., 1933. A simplified method of staining endospores. Science 77, 194.
Serrano, M., Real, G., Santos, J., Carneiro, J., Moran Jr., C.P., Henriques, A.O., 2011. A negative feedback loop that limits the ectopic activation of a cell type–specific sporulation sigma factor of *Bacillus subtilis*. PLOS Genet. 7, e1002220.
Spuhler, D., Rengifo-Herrera, J.A., Pulgarin, C., 2010. The effect of Fe^{2+}, Fe^{3+}, H_2O_2 and the photo-Fenton reagent at near neutral pH on the solar disinfection (SODIS) at low temperatures of water containing *Escherichia coli* K12. Appl. Catal. B 96, 126–141.
Stadler, J.A., Schweyen, R.J., 2002. The yeast iron regulon is induced upon cobalt stress and crucial for cobalt tolerance. J. Biol. Chem. 277, 39649–39654.
Tyrrell, R., Pourzand, C., Brown, J., Hejmadi, V., Kvam, E., Ryter, S., Watkin, R., 2000. Cellular studies with UVA radiation: a role for iron. Radiat. Prot. Dosim. 91, 37–39.
Ullmann, B.D., Myers, H., Chiranand, W., Lazzell, A.L., Zhao, Q., 2004. Inducible defense mechanism against nitric oxide in *Candida albicans*. EC 3, 715–723.
United States Environmental Protection Agency, 1993. Method 410.4. The Determination of Chemical Oxygen Demand by Semi-automated Colorimetry.
Venieri, D., Gounaki, I., Binas, V., Zachopoulos, A., Kiriakidis, G., Mantzavinos, D., 2015. Inactivation of MS2 coliphage in sewage by solar photocatalysis using metal-doped TiO_2. Appl. Catal. B Environ. 178, 54–64.
Wang, X., Yi, M., Liu, H., Han, Y., Yi, H., 2017. Reactive oxygen species and Ca^{2+} are involved in cadmium-induced cell killing in yeast cells. Can. J. Microbiol. 63, 153–159.
Wang, Y.R., Chu, W., 2012. Photo-assisted degradation of 2,4,5-trichlorophenoxyacetic acid by Fe(II)-catalyzed activation of Oxone process: the role of UV irradiation, reaction mechanism and mineralization. Appl. Catal. B 123–124, 151–161.
Wang, Z.H., Yuan, R.X., Guo, Y.G., Xu, L., Liu, J.S., 2011. Effects of chloride ions on bleaching of azo dyes by Co^{2+}/oxone reagent: kinetic analysis. J. Hazard. Mater. 190, 1083–1087.
Wei, G., Liang, X., He, Z., Liao, Y., Xie, Z., Liu, P., Ji, S., He, H., Li, D., Zhang, J., 2015. Heterogeneous activation of Oxone by substituted magnetites Fe_3−xMxO_4 (Cr, Mn, Co, Ni) for degradation of Acid Orange II at neutral pH. J. Mol. Catal. A. Chem. 398, 86–94.
World Health Organization, 2008. Guidelines for Drinking-water Quality. Geneve (Switzerland).
Yu, Z.Y., Kiwi-Minsker, L., Renken, A., Kiwi, J., 2006. Detoxification of diluted azo-dyes at biocompatible pH with the Oxone/Co^{2+} reagent in dark and light processes. J. Mol. Catal. A. Chem. 252, 113–119.